HHS Public Access

Author manuscript

ACS Biomater Sci Eng. Author manuscript; available in PMC 2018 August 14.

Published in final edited form as:

ACS Biomater Sci Eng. 2017 August 14; 3(8): 1641–1653. doi:10.1021/acsbiomaterials.7b00166.

Synthesis and Application of Injectable Bioorthogonal Dendrimer Hydrogels for Local Drug Delivery

Leyuan Xu[1,2,#], **Remy C. Cooper**[3,#], **Juan Wang**[1], **W. Andrew Yeudall**[4,5], and **Hu Yang**[1,6,7,*]

[1]Department of Chemical and Life Science Engineering, Virginia Commonwealth University, 737 North 5th Street, Richmond, Virginia 23219, United States

[3]Department of Biomedical Engineering, 601 West Main Street, Virginia Commonwealth University, Richmond, Virginia 23284, United States

[4]Department of Oral Biology, Augusta University, 1120 15th Street, Augusta, Georgia 30912, United States

[5]Molecular Oncology and Biomarkers Program, Georgia Cancer Center, 1410 Laney Walker Blvd, Augusta University, Augusta, Georgia 30912, United States

[6]Department of Pharmaceutics, Virginia Commonwealth University, 410 North 12th Street, Richmond, Virginia 23298, United States

[7]Massey Cancer Center, Virginia Commonwealth University, 401 College Street, Richmond, Virginia 23298, United States

Abstract

We developed novel dendrimer hydrogels (DH)s on the basis of bioorthogonal chemistry, in which polyamidoamine (PAMAM) dendrimer generation 4.0 (G4) functionalized with strained alkyne dibenzocyclooctyne (DBCO) via PEG spacer (M_n = 2,000 g/mol) underwent strain-promoted azide-alkyne cycloaddition (SPAAC) with polyethylene glycol bisazide (PEG-BA) (M_n= 20,000 g/mol) to generate a dendrimer-PEG cross-linked network. This platform offers a high degree of functionality and modularity. A wide range of structural parameters including dendrimer generation, degree of PEGylation, loading density of clickable DBCO groups, PEG-BA chain length as well as the ratio of clickable dendrimer to PEG-BA and their concentrations can be readily manipulated to tune chemical and physical properties of DHs. We used this platform to prepare an injectable liquid DH. This bioorthogonal DH exhibited high cytocompatibility and enabled sustained release of the anticancer drug 5-fluorouracil (5-FU). Following intratumoral injection, the DH/5-FU formulation significantly suppressed tumor growth and improved survival of HN12 tumor-bearing mice by promoting tumor cell death as well as by reducing tumor cell proliferation and angiogenesis.

[*]**Corresponding Author:** hyang2@vcu.edu.

[2]Current address: Department of Internal Medicine, Yale University, 330 Cedar Street, New Haven, Connecticut 06520

[#]The authors contributed equally to the work.

ORCID

Hu Yang: 0000-0003-3030-004X

Author Contributions

The manuscript was written through contributions of all authors. All authors have given approval to the final version of the manuscript.

TOC image

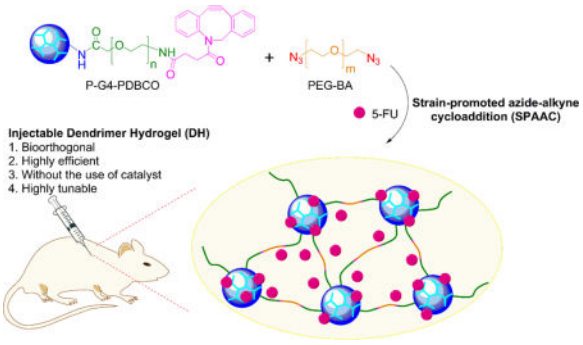

Keywords

nanomedicine; hydrogel; local drug delivery; chemotherapy; copper-free click chemistry

1. Introduction

Dendrimers have been actively studied for developing targeted cancer therapies by virtue of their well-defined nanoscale structural features and properties.[1–8] Using dendrimers and hyperbranched polymers as building blocks to synthesize hydrogels has attracted much attention for various applications.[9–13] For instance, dendrimer hydrogels (DHs) on the basis of polycationic full generation and polyanionic half-generation polyamidoamine (PAMAM) dendrimers have been synthesized successfully using photoinitiated polymerization.[14–15] The DHs integrate structural characteristics and properties of dendrimer nanoparticles and PEG networks. Although free radicals produced by photoinitiators are necessary for the reaction, they, along with unreacted residues, may deactivate intracellular signaling pathways critical for cell survival such as the AKT signaling pathway.[16]

To ease safety concerns about the use of photoinitiators and make more biocompatible dendrimer hydrogel formulations, we applied copper-free click chemistry to develop novel bioorthogonal DHs. In this new design, we functionalized polyamidoamine (PAMAM) dendrimer generation 4.0 (G4) with strained alkyne, i.e., dibenzocyclooctyne (DBCO), to obtain “clickable” dendritic macromonomers. Upon mixing of DBCO-containing dendritic macromonomer with polyethylene glycol bisazide (PEG-BA) in water, DBCO and azide undergo strain-promoted azide-alkyne cycloaddition (SPAAC) to generate a dendrimer-PEG cross-linked network rapidly at room temperature in the absence of catalysts. Different from our early DHs that are prepared on the basis of intermolecular cross-linking of dendrimer-PEG acrylate, dendrimers are loosely knotted by long PEG chains in this new type of DHs. Because of this new structural feature, the structure and properties of the formed DHs can be more readily modulated. Herein, we describe the synthesis and characterization of DHs prepared based on bioorthogonal chemistry. We coupled DBCO directly to G4 or to a PEG spacer (M_n = 2,000 g/mol) and then grafted PEGylated DBCO to G4 to form clickable dendritic macromonomer G4-DBCO or P-G4-PDBCO, respectively. Either G4-DBCO or P-G4-PDBCO reacted with long PEG-BA (M_n = 20,000 g/mol) following SPAAC to form DH-G4-DBCO or DH-P-G4-PDBCO, respectively. Perhaps a striking feature of the

resulting bioorthogonal DH-P-G4-PDBCO is its ability to form gels while maintaining fluidity. The fluidity was utilized to prepare an injectable drug formulation for local drug delivery.

To prove our concept, we tested this new platform in a xenograft mouse model of head and neck cancer. Fluorouracil (5-FU), a chemotherapeutic agent commonly prescribed for head and neck cancer, was used as a model compound. Head and neck squamous cell carcinomas (HNSCC) account for approximately 3% of all cancers, and the mortality of head and neck cancers is estimated at about 22% in the United States.[17] Chemotherapy remains one of the standard treatments for head and neck cancers but may lead to severe toxicity.[18–19] Because of the specific location of head and neck cancers, i.e., the oral and oropharyngeal region, the tumors are relatively accessible. Thus, local administration of chemotherapeutics, i.e., intratumoral (i.t.) administration and convection-enhanced delivery (CED), has been found to be more efficacious than conventional systemic chemotherapy.[20] The antitumor efficacy of this new drug formulation was tested and confirmed for local drug delivery in a xenograft mouse model of head and neck cancer.

2. Materials and Methods

2.1. Materials

Diaminobutane (DAB)-core PAMAM dendrimer generation 4.0 (G4) was purchased from NanoSynthons (Mt. Pleasant, MI). DBCO-NHS ester was purchased from Click Chemistry Tools (Scottsdale, AZ). 5-Fluorouracil (5-FU), dimethyl sulfoxide (DMSO), deuterium oxide (D_2O, 99.9 atom % D), 4-(4,6-Dimethoxy-1,3,5-triazin-2-yl)-4-methylmorpholinium chloride (DMTMM), polyethylene glycol bisazide (PEG-BA, M_n=20,000 g/mol), trifluoroacetic acid (TFA), and formaldehyde solution (37 wt. % in H_2O) were purchased from Sigma-Aldrich (St. Louis, MO). Acetonitrile (ACN), water (HPLC grade), hydrogen peroxide (H_2O_2), and phosphate-buffered saline (PBS) were purchased from Fisher Scientific (Pittsburgh, PA). NH_2-PEG-COOH (M_n = 2000 g/mol) was purchased from JenKem Technology USA (Plano, TX). SnakeSkin dialysis tubing (molecular weight cut-off (MWCO) = 3500 or 7000 daltons) was purchased from Thermo Scientific (Rockford, IL). Vectastain ABC kit, 3,3′-diaminobenzidine (DAB), and hematoxylin were purchased from Vector Laboratories (Burlingame, CA). BD Retrievagen Antigen Retrieval Systems were purchased from BD Biosciences (San Jose, CA). Ki67, cleaved caspase-3 (Asp175) and apoptosis-inducing factor (AIF) antibodies were purchased from Cell Signaling Technology (Danvers, MA). CD31 antibody was purchased from Abcam (Cambridge, MA). Dulbecco's modified Eagle medium (DMEM), trypsin-EDTA (0.25%), and penicillin-streptomycin (10,000 U/mL) were purchased from Life Technologies (Carlsbad, CA). Cosmic calf serum (CS) was purchased from Lonza (Walkersville, MD). Cell proliferation reagent WST-1 was purchased from Roche Applied Science (Grand Island, NY).

2.2. Synthesis of "clickable" dendritic macromonomers

As shown in Scheme 1, G4-DBCO macromonomer was synthesized by directly coupling DBCO to G4. Briefly, DBCO-NHS (6.9 mg, 17.1 μmol, MW = 402.4 g/mol) was dissolved in 2.3 mL of DMSO and then added dropwise to 8 mL of $NaHCO_3$ solution (pH 8)

containing PAMAM dendrimer G4 (24.5 mg, 1.7 μmol, MW = 14215 g/mol). The reaction mixture was stirred for one day and then dialyzed against DI water using dialysis tubing (MWCO = 7,000 Da) for 2 days.

As shown in Scheme 2, P-G4-PDBCO macromonomer was synthesized by PEGylating DBCO to form PDBCO and then grafting PDBCO to G4 along with PEG. Briefly, DBCO-NHS (6.9 mg, 17.1 μmol, MW = 402.4 g/mol) was dissolved in 2.3 mL of DMSO, added dropwise to 5.7 mL of $NaHCO_3$ solution (pH 8) containing NH_2-PEG-COOH (51.6 mg, 25.9 μmol, M_n = 2000 g/mol). The reaction mixture was stirred overnight at room temperature. The reaction mixture was then added dropwise to 8 mL of $NaHCO_3$ solution (pH 8) containing PAMAM dendrimer G4 (24.5 mg, 1.7 μmol) and DMTMM (14.3 mg, 51.8 μmol, MW = 276.7 g/mol). The reaction mixture was stirred for 24 h and then dialyzed against DI water using dialysis tubing (MWCO = 7,000 Da) for 2 days.

The resultant G4-DBCO and P-G4-PDBCO conjugates were obtained after lyophilization and characterized by ultraviolet–visible (UV-Vis) spectroscopy, proton nuclear magnetic resonance (^{1}H NMR) spectroscopy and high performance liquid chromatography (HPLC).

2.3. Instrumentation

^{1}H NMR spectra were recorded on a Varian superconducting Fourier-transform NMR spectrometer (Mercury-300) in the Nuclear Magnetic Resonance Center at Virginia Commonwealth University. D_2O was used as the solvent. The reverse-phase HPLC system (Waters, Milford, MA) consisting of a system Waters 1515 isocratic HPLC pump, a model Waters 717plus autosampler, a model Waters 2487 dual λ absorbance detector, and an XTerra particle-based RP-HPLC column (length 150 mm, particle size 5 μm, RP18, Milford, MA) was used in this work. The mobile phase was H_2O:ACN:TFA (500:500:0.38, v/v/v) at a flow rate of 1 mL/min. The analysis was performed using the Breeze™ software (Waters, Milford, MA).

2.4. Preparation of bioorthogonal dendrimer hydrogels (DHs) and injectable liquid DH/5-FU formulation

Bioorthogonal DH-G4-DBCO was prepared by mixing equal volumes of G4-DBCO (20 mg/mL) and PEG-BA (50 mg/mL) for 30 min as shown in Scheme 1. Bioorthogonal DH-P-G4-PDBCO was prepared by mixing equal volume of P-G4-PDBCO aqueous solution (100 mg/mL) and PEG-BA aqueous solution (100, 500, or 1000 mg/mL) for 30 min as shown in Scheme 2. The freshly prepared DH-G4-DBCO and DH-P-G4-PDBCO were subjected to rheological testing, morphological evaluation, and cytotoxicity assessment.

DH-P-G4-PDBCO with P-G4-PDBCO to PEG-BA ratio of 1/10, simplified as DH afterwards, was chosen for in vitro drug release and in vivo drug delivery evaluation. Briefly, DH/5-FU was prepared in situ by dissolving appropriate amounts of 5-FU in the mixture of P-G4-PDBCO and PEG-BA solution simultaneously. The quantity of the loaded 5-FU was 5 mg on the basis of P-G4-PDBCO (10 mg) and PEG-BA (100 mg). Plain and drug-loaded DHs were prepared immediately before each test.

2.5. Rheological testing

Rheological testing was performed using a 20 mm diameter disk on a temperature controlled plate of an HR-3 Discovery Hybrid Rheometer (TA instruments, New Castle, DE). Each set of samples on the plate at 25 °C was subjected to compression and shear stress by a 20 mm diameter parallel plate. An amplitude sweep was performed to ensure that all the measurements were conducted within the linear viscoelastic region. Oscillatory frequency sweeps were then carried out with a constant strain of 1% in the frequency region of 0.1–100 rad/s.[21]

2.6. Morphology examination

DHs were lyophilized and mounted on an aluminum stub and sputter-coated with platinum for 1 min. The scanning electron microscopy (SEM) images of dendrimer hydrogels were taken under a JEOL LV-5610 scanning electron microscope at 20 kV.

2.7. Drug release study

Free 5-FU (600 μg) or DH containing 600 μg of 5-FU in PBS (pH7.4) was transferred into a dialysis tube (MWCO = 500–1000 Da). The dialysis tube was soaked in 50 mL of PBS at room temperature. At the pre-determined time points (0 min, 15 min, 30 min, 2 h, 3 h, 4 h, 6 h , and 12 h), an aliquot (500 μL) was withdrawn from outside the dialysis tube and replaced with an equal amount of fresh PBS. The withdrawn samples were analyzed using an isocratic HPLC method with a UV detector at the wavelength of 260 nm. Standards for 5-FU (1–200 μg/mL) were prepared in PBS (pH 7.4) and subjected to HPLC analysis where flow rate was set at 1 mL/min to establish a standard curve. Cumulative release of 5-FU from the hydrogel was then determined following a reported method.[22]

2.8. Cell culture

HN12 cells, derived from an HNSCC lymph node metastasis, and NIH3T3 fibroblasts were cultured as described previously in Dulbecco's modified Eagle's medium (DMEM) supplemented with 10% Cosmic calf serum, 100 units/mL of penicillin, and 100 μg/mL of streptomycin at 37 °C in 95% air/5% CO_2 as previously described.[23]

2.9. Cytotoxicity assay

HN12 cells or NIH3T3 fibroblasts were seeded at a density of 1×10^4 cells per well in a 96-well plate and cultured for 1 day to allow cell attachment. The cells were then treated with 5-FU (0–10 mM), DH-G4-DBCO or DH-P-G4-PDBCO (0–6 mg/mL) at various concentrations for 2 days. Cell viability relative to untreated cells was then determined by WST-1 proliferation assay. The four parameters logistic regression was used to perform the curve fitting and then determine the 50% maximal inhibitory concentrations (IC_{50}) of free 5-FU.[24]

2.10. Animal studies

Animal studies were approved by the Institutional Animal Care and Use Committee (IACUC) of Virginia Commonwealth University. HN12 cells (5×10^6 cells) were injected subcutaneously (s.c.) into the right flank of 4-week-old female athymic nude mice (Harlan

Sprague Dawley, Indianapolis, IN). When the tumors had developed to a volume of 100 mm^3 (V_0) on average at 6 days post-injection, the mice were randomly divided into 4 groups in a way to minimize tumor size and body weight differences among the groups. The mice from each group were injected i.t. with PBS, DH (110 mg/kg), DH/5-FU [(110 mg/5 mg/kg)], or free 5-FU (5 mg/kg),[25–26] respectively, at the center of the tumor every 4 days. During the treatment, body weight was monitored, and tumor size was measured by standard digital caliper (Tresna, Guangxi Province, China) every other day. The tumor volume was calculated using the formula Volume= (Length × $Width^2$)/2, with the Width being smaller than the Length. Mice were euthanized at the end of the experiment, or when signs of discomfort/ulceration were detected by the investigator, or as recommended by the veterinarian who monitored the mice daily.[27] A tumor volume of 500 mm^3 was used as a threshold value to report animal survival rate following the same strategy as described previously.[28–29] At the end of the treatment, the tumor was collected from surviving mice and fixed in 10% neutral-buffered formalin for histologic evaluation.

2.11. Hematoxylin and eosin (H&E) staining

The formalin-fixed tumor specimens were embedded in paraffin and sectioned at 5 μm. The H&E staining was performed at the VCU Massey Cancer Biological Macromolecule Core Facility. The tissues slides were imaged under a Nikon microscope (Nikon Instruments Inc., Melville, NY) using a magnification of 200×.

2.12. Immunohistochemistry (IHC)

The IHC staining was carried out following procedures described previously[30]. Briefly, the formalin-fixed tumor specimens were embedded in paraffin, and sectioned at 5 μm, deparaffinized in xylene, and rehydrated in graded alcohols (100%, 95%, 90%, 80%, and 70%). For antigen retrieval, the sections were microwaved in antigen retrieval buffer for 10 min. Endogenous peroxidase activity was quenched by incubation in 3% (v/v) H_2O_2 for 15 min. The sections were incubated with the primary polyclonal antibody against cleaved caspase-3, AIF, Ki67, or CD31 for 1 h. After the sections were washed with TBS, the immobilized antibodies were detected using a Vectastain ABC kit (Vector Laboratories, Burlingame, CA). DAB and hematoxylin were used as the chromogen and the nuclear counterstain, respectively. The primary antibody was omitted as negative control. The tissues slides were then imaged under a Nikon Ti-U microscope using a magnification of 200×. The cleaved caspase-3^{high}, AIF-positive, and CD31-positive area percentages or Ki67-positive cell percentage (index) were quantitated from 8–9 randomly selected fields for each sample, and each group included sections from 3 mice.

2.13. Statistical analysis

The data were expressed as means ± standard deviation (SD). The data were analyzed using one-way analysis of variance (ANOVA) followed by Holm-Sidak method for subgroup comparison. A value of $p < 0.05$ was considered statistically significant.

3. Results

3.1. Preparation and characterization of the bioorthogonal DH

In this design, DBCO was covalently directly coupled to PAMAM dendrimer G4 or via a PEG spacer to reduce steric crowding. Extra PEG chains were also coupled to the dendrimer surface to improve cytocompatibility. The obtained clickable DBCO-containing dendritic macromonomers G4-DBCO and P-G4-PDBCO were characterized with UV-Vis, HPLC and ^{1}H NMR spectroscopy. In the UV-Vis spectrum, DBCO-NHS showed two absorbance peaks at 220 nm and 290 nm whereas G4 shows only one absorbance peak at 220 nm (Figure 1A). The UV-Vis spectra of both G4-DBCO and P-G4-PDBCO showed an absorbance peak at 290 nm in addition to an absorbance peak of dendrimer, indicating the presence of DBCO in the resultant conjugates. Additionally, we were able to distinguish P-G4-PDBCO from G4 by tracking its DBCO component at the wavelength of 290 nm using HPLC equipped with a UV detector. According to the HPLC chromatogram, DBCO-NHS has a retention time of 1.8 min (Figure 1B). Both G4-DBCO and P-G4-PDBCO have a retention time of 1.1 min. By calculating the area under the curve (AUC), the purity of G4-DBCO and P-G4-PDBCO was determined to be 99.7% and 94.6%, respectively. Lastly, the ^{1}H NMR spectrum (Figure 1C) confirms the presence of the benzene protons of DBCO (proton peaks between 7.0 and 7.7 ppm), methylene protons of G4 branches (proton peaks between 2.1 and 3.6 ppm), and methylene protons of PEG repeat units (3.7 ppm). According to NMR integration, G4-DBCO carried an average of 7 DBCO per dendrimer; whereas P-G4-PDBCO carried an average of 5 PDBCO and 7 PEG chains per dendrimer.

Bioorthogonal dendrimer hydrogel, DH-G4-DBCO, was obtained by reacting G4-DBCO with PEG-BA at a weight ratio of 1/2.5 in water; whereas DH-P-G4-PDBCO was obtained by reacting P-G4-PDBCO with PEG-BA at weight ratios of 1/1, 1/5, and 1/10 in water. All formulated dendrimer hydrogels remained in liquid form and showed gel properties as confirmed by rheological testing. An amplitude sweep was performed first to determine the linear viscoelastic region (LVR) (Figure 2A). The frequency sweeps were then conducted at a fixed strain of 1%, which was within the LVR. It displayed typical hydrogel viscoelastic behavior as its storage modulus (G') was higher than its loss modulus (G'') with frequency-independence (Figure 2B). The highly porous structure of the resulting dendrimer hydrogels was illustrated by SEM (Figure 2C). The apparent pore diameters of the resulting dendrimer hydrogels were determined in a micrometer scale range based on SEM images (Figure 2D). Given that such a loosely cross-linked hydrogel afforded excellent drug-loading capacity, controlled release property and was injectable, we moved forward with a particular formulation, i.e., DH-P-G4-PDBCO, referred to as DH, for local drug delivery.

3.2. In vitro assessment of DH-P-G4-PDBCO

PEGylation has been well documented to reduce toxicity and immunogenicity of dendritic nanoparticles or prodrugs.[31] PEG used as a spacer and cross-linker constitutes a significant portion of the DH-P-G4-PDBCO. According to the WST-1 assay, DH-P-G4-PDBCO shows a higher cytocompatibility with both human head and neck cancer cells (HN12) and mouse fibroblasts (NIH3T3) than DH-G4-DBCO (Figure 3).

5-FU is an active chemotherapeutic agent for treatment of head and neck cancers. We first validated the cytotoxicity of 5-FU in synchronous lymph node metastasis-derived HN12 cells. It was found that 5-FU dose-dependently decreased the viability of HN12 cells with an IC_{50} of 44.5 μM (Figure 4A). In vitro drug release kinetics from nanoparticle or hydrogel generally exhibits two phases, i.e., burst release phase and sustained release phase.[22, 24] Burst release allows the drug to rapidly reach an effective concentration, whereas sustained release allows the drug to stay at an effective concentration in the circulation over time. Due to the good solubility of 5-FU (1 mg/mL), over 80% of 5-FU was diffused out of the dialysis bag within 2 h and reached a complete diffusion (100%) within 6 h (Figure 4B). In contrast, an initial burst release of 5-FU was observed in the DH/5-FU group, followed by an extended release up to 12 h.

3.3. In vivo antitumor effects of DH/5-FU

The antitumor effect of DH/5-FU was evaluated in a xenograft mouse model of head and neck cancer. Repeated intratumoral injection of 5-FU inhibited tumor growth initially but failed to suppress the tumor growth after the treatment was stopped at day 12 (Figure 5A). DH alone did not show an effect on tumor growth. In contrast, DH/5-FU significantly suppressed tumor growth up to 18 days, presumably due to the sustained release of 5-FU from DH. As a result, DH/5-FU improved mouse survival rate compared to the PBS, DH, and 5-FU groups (Figure 5B). No difference in mouse body weight or any other discomfort was observed during the DH/5-FU treatment (Figure 5C), indicating DH's good tissue compatibility.

Upon the termination of the experiment, the tumor tissues were collected and assessed histologically for evidence of antitumor effects. The H&E staining did not show any toxicity effect in the tumors treated with DH alone (Figure 6). 5-FU exerts antitumor activity by inhibiting proliferation, inducing cell apoptosis, and suppressing tumor angiogenesis.[32–34] We conducted IHC staining of tumor tissue sections using four different markers, i.e., Ki67 (Figure 7), CD31 (Figure 8), cleaved caspase-3 (Figure 9), and AIF (Figure 10). Quantification of these biomarkers showed that DH/5-FU and free 5-FU exhibited equivalent potency and significantly inhibited tumor cell proliferation and reduced tumor angiogenesis ($p<0.001$). More impressively, DH/5-FU was the only group that was capable of inducing cell apoptosis, as judged by both cleaved caspase-3 and AIF staining. Collectively, our studies demonstrate that DH/5-FU was more potent than the 5-FU group in exerting antitumor effects.

4. Discussion

In the last decade, a tremendous effort has been made to develop localized drug delivery technologies, including polymer-drug conjugates, nanoparticles, and hydrogels. Among these formulations, injectable hydrogels appear to be compelling in that they provide a controlled and sustained drug release at the local tumor site, increase drug solubility and bioavailability, and reduce adverse systemic effects.[35–36] A variety of in-situ depot-forming hydrogels have been developed for localized drug delivery.[20, 35] Several hydrogel

formulations, such as PEG-PCL-PEG hydrogel and silk-elastin-like hydrogel, have been reported to enhance drug and gene delivery for the treatment of head and neck cancers.[37–39]

In this work, we successfully synthesized two “clickable” dendritic macromonomers, G4-DBCO and P-G4-PDBCO (Figure 1). Both G4-DBCO and P-G4-PDBCO were able to cross-link with PEG-BA to form bioorthogonal dendrimer hydrogels with a highly porous microstructure and viscoelastic properties (Figure 2). More interestingly, we found the modulus of DH-P-G4-PDBCO increased as the weight ratio of PEG-BA to P-G4-PDBCO increased. Despite the fact that DH-G4-DBCO showed hydrogel properties, we found that extra PEGylated DH-P-G4-PDBCO was more suitable for developing an injectable local drug delivery platform for multiple reasons: 1) PEG serves as a spacer between dendrimer and DBCO, which may help to reduce steric crowding. 2) PEGylated P-G4-PDBCO improves solubility of DBCO-conjugated dendrimer. 3) Extra PEG improves cytocompatibility of dendrimer hydrogel (Figure 3). 4) PEGylation helps to reduce nonspecific cellular uptake of polycationic dendrimer G4. 5) More PEGylated dendrimers can be cleared through the circulation to reduce local toxicity at later stages after injection. 6) Liquid DH-P-G4-PDBCO is suitable for injection without blocking the needle. As opposed to P-G4-PDBCO, G4-DBCO lacks the PEG spacer and tends to form a more compact network, which is more resistant to deformation.

We found that DH/5-FU exhibited two-phase in vitro release kinetics, i.e., a burst release phase and a sustained release phase, which can be explained as follows. The pore size of DH in the dry state was about 15 μm in diameter (Figure 2D). When immersed in aqueous solution, DH is expected to swell, and its pore size tends to increase. Small molecular-weight drugs such as 5-FU, which are loosely entrapped in the DH network, are expected to diffuse out freely through the interconnected pores, causing a burst drug release. However, those 5-FU molecules entrapped within dendrimers via electrostatic and hydrophobic interaction may be released at a much slower rate.[40–41] Through these two release mechanisms, DH is expected to provide a sufficient initial release of 5-FU and a more sustained release afterwards to maintain a high drug concentration at the tumor site after local injection, compared to the free 5-FU. However, the DH/5-FU formulation needs to be optimized depending on demand. As proof-of-concept, our animal studies confirmed that DH/5-FU significantly suppressed tumor growth by inducing tumor apoptosis and inhibiting tumor cell proliferation and angiogenesis. The survival of HN12 tumor-bearing mice treated with DH/5-FU was significantly extended as a result.

Most systems require photo-polymerization, e.g., photocrosslinkable chitosan (Az-CH-LA) and PEG dimethacrylate (PEG-DMA) hydrogel,[42–43] or chemical catalysts, e.g., genipin,[44] for cross-linking. Photo-polymerized hydrogels yield great stability and excellent mechanical properties, but need to be triggered by external light, e.g., UV light, which can produce free radicals, induce cellular reactive oxygen species (ROS) formation, and subsequently reduce biocompatibility of hydrogels. Chemically cross-linked hydrogels display great stability and elasticity, albeit at a slow cross-linking rate, and the presence of cross-linkers can be toxic to the surrounding tissues. Physically cross-linked hydrogels can avoid chemical reaction, but the mechanical instability is an issue.[45] Unlike these traditional cross-linking hydrogel approaches, our DH formulation is based on bioorthogonal “click”

chemistry. It allows rapid reaction without any catalysts and minimal interference with a biological system.[46–47] By tuning a wide range of structural parameters including dendrimer generation, degree of PEGylation, loading density of clickable DBCO groups, PEG-BA chain length as well as ratio of clickable dendrimer to PEG-BA and their concentrations, we can alter the viscoelastic properties of DHs to meet the needs of various applications, e.g., injection routes, implantation, local microenvironment, and so on. In light of the highly efficient reaction rates, it would be interesting to test whether we can synergistically inject drug-loaded dendrimer-DBCO conjugates with PEG-BA to form hydrogel at the tumor site, perhaps enabling better tissue penetration and retention. Another strategy of depot-forming hydrogels is based on in-situ phase separation, which can be induced by changing the solubility of the polymer with respect to induction of pH,[48] temperature,[49–50] ultrasound,[51] or radiation.[52] Due to the acidic tumor microenvironment of head and neck cancers, it is desirable to incorporate pH-sensitive linkages, e.g., ester linkage, or thermo-sensitive linkages into DH formulations. It will not only release chemotherapeutic agents but disintegrate the drug-loaded dendrimer cargos in a synergistic manner. Additionally, we have previously described that our DH network allows for simultaneous delivery of both hydrophobic and hydrophilic drugs as needed.[15] The interior hydrophobic core of the dendrimers can encapsulate hydrophobic drugs to increase their solubility and loading dose. On the other hand, hydrophilic drugs can be loaded in the PEG network. The polycationic surface of full generation PAMAM dendrimers can complex with negatively-charged drugs or genetic materials. Overall, the DHs possess unique structural characteristics and tunable properties to meet various drug delivery needs and allow for combination chemotherapy. The aforementioned strategies will be explored to design more efficient injectable formulations for localized drug delivery.

5. Conclusions

We designed and developed novel injectable bioorthogonal dendrimer hydrogels on the basis of bioorthogonal chemistry. This platform offers a high degree of functionality and modularity. A wide range of structural parameters including dendrimer generation, degree of PEGylation, loading density of clickable DBCO groups, PEG-BA chain length as well as ratio of dendrimer to PEG-BA can be readily manipulated to tune chemical and physical properties of dendrimer hydrogels. In particular, the injectable bioorthogonal DH prepared under the conditions described in this work exhibited high cytocompatibility and sustained drug release. It was used to fabricate an injectable formulation for sustained release and localized delivery of the anticancer drug 5-FU. The DH/5-FU formulation significantly suppressed tumor growth and improved animal survival of HN12 tumor-bearing mice by promoting cancer cell death as well as by reducing cancer cell proliferation and tumor angiogenesis.

Acknowledgments

This work was supported, in part, by the National Science Foundation (CAREER award CBET0954957) and the National Institutes of Health (R01EY024072 and R01DE024381).

References

1. Tomalia DA, Baker H, Dewald J, Hall M, Kallos G, Martin S, Roeck J, Ryder J, Smith P. A new class of polymers: starburst-dendritic macromolecules. Polym J (Tokyo). 1985; 17(1):117–32.
2. Bosman AW, Janssen HM, Meijer EW. About Dendrimers: Structure, Physical Properties, and Applications. Chem Rev (Washington, DC US). 1999; 99(7):1665–1688.
3. Vogtle F, Gestermann S, Hesse R, Schwierz H, Windisch B. Functional dendrimers. Prog Polym Sci. 2000; 25(7):987–1041.
4. Xu L, Zhang H, Wu Y. Dendrimer advances for the central nervous system delivery of therapeutics. ACS Chem Neurosci. 2014; 5(1):2–13. [PubMed: 24274162]
5. Yang H. Targeted nanosystems: Advances in targeted dendrimers for cancer therapy. Nanomedicine. 2016; 12(2):309–16. [PubMed: 26706410]
6. Yang H, Kao WJ. Dendrimers for pharmaceutical and biomedical applications. J Biomater Sci Polym Ed. 2006; 17(1-2):3–19. [PubMed: 16411595]
7. Xu, L., Yang, H. Handbook of Nanobiomedical Research. WORLD SCIENTIFIC; 2014. Nanopreparations for Central Nervous System Diseases; p. 203-230.
8. Xu, L., Yeudall, WA., Yang, H. Tailored Polymer Architectures for Pharmaceutical and Biomedical Applications. Vol. 1135. American Chemical Society; 2013. Dendrimer-Based RNA Interference Delivery for Cancer Therapy; p. 197-213.
9. Carnahan MA, Middleton C, Kim J, Kim T, Grinstaff MW. Hybrid dendritic-linear polyester-ethers for in situ photopolymerization. J Am Chem Soc. 2002; 124(19):5291–5293. [PubMed: 11996569]
10. Sontjens SH, Nettles DL, Carnahan MA, Setton LA, Grinstaff MW. Biodendrimer-based hydrogel scaffolds for cartilage tissue repair. Biomacromolecules. 2006; 7(1):310–6. [PubMed: 16398530]
11. Ghobril C, Rodriguez EK, Nazarian A, Grinstaff MW. Recent Advances in Dendritic Macromonomers for Hydrogel Formation and Their Medical Applications. Biomacromolecules. 2016; 17(4):1235–52. [PubMed: 26978246]
12. Zhang H, Patel A, Gaharwar AK, Mihaila SM, Iviglia G, Mukundan S, Bae H, Yang H, Khademhosseini A. Hyperbranched polyester hydrogels with controlled drug release and cell adhesion properties. Biomacromolecules. 2013; 14(5):1299–310. [PubMed: 23394067]
13. Navath RS, Menjoge AR, Dai H, Romero R, Kannan S, Kannan RM. Injectable PAMAM dendrimer-PEG hydrogels for the treatment of genital infections: formulation and in vitro and in vivo evaluation. Mol Pharm. 2011; 8(4):1209–23. [PubMed: 21615144]
14. Desai PN, Yuan Q, Yang H. Synthesis and characterization of photocurable polyamidoamine dendrimer hydrogels as a versatile platform for tissue engineering and drug delivery. Biomacromolecules. 2010; 11(3):666–73. [PubMed: 20108892]
15. Holden CA, Tyagi P, Thakur A, Kadam R, Jadhav G, Kompella UB, Yang H. Polyamidoamine dendrimer hydrogel for enhanced delivery of antiglaucoma drugs. Nanomedicine. 2012; 8(5):776–83. DOI: 10.1016/j.nano.2011.08.018. [PubMed: 21930109]
16. Xu L, Sheybani N, Yeudall WA, Yang H. The effect of photoinitiators on intracellular AKT signaling pathway in tissue engineering application. Biomater Sci. 2015; 3(2):250–255. [PubMed: 25709809]
17. Jemal A, Siegel R, Xu J, Ward E. Cancer statistics, 2010. CA Cancer J Clin. 2010; 60(5):277–300. [PubMed: 20610543]
18. Forastiere AA, Goepfert H, Maor M, Pajak TF, Weber R, Morrison W, Glisson B, Trotti A, Ridge JA, Chao C, Peters G, Lee D-J, Leaf A, Ensley J, Cooper J. Concurrent Chemotherapy and Radiotherapy for Organ Preservation in Advanced Laryngeal Cancer. New England Journal of Medicine. 2003; 349(22):2091–2098. [PubMed: 14645636]
19. Tsao AS, Garden AS, Kies MS, Morrison W, Feng L, Lee JJ, Khuri F, Zinner R, Myers J, Papadimitrakopoulou V, Lewin J, Clayman GL, Ang KK, Glisson BS. Phase I/II study of docetaxel, cisplatin, and concomitant boost radiation for locally advanced squamous cell cancer of the head and neck. J Clin Oncol. 2006; 24(25):4163–9. [PubMed: 16943532]
20. Fakhari A, Subramony JA. Engineered in-situ depot-forming hydrogels for intratumoral drug delivery. J Control Release. 2015; 220(Pt A):465–75. [PubMed: 26585504]

21. Wang J, He H, Cooper RC, Yang H. In Situ-Forming Polyamidoamine Dendrimer Hydrogels with Tunable Properties Prepared via Aza-Michael Addition Reaction. ACS applied materials & interfaces. 2017; 9(12):10494–10503. [PubMed: 28263553]
22. Li S, Wang A, Jiang W, Guan Z. Pharmacokinetic characteristics and anticancer effects of 5-fluorouracil loaded nanoparticles. BMC Cancer. 2008; 8:103. [PubMed: 18412945]
23. Xu L, Kittrell S, Yeudall WA, Yang H. Folic acid-decorated polyamidoamine dendrimer mediates selective uptake and high expression of genes in head and neck cancer cells. Nanomedicine (Lond). 2016; 11(22):2959–2973. [PubMed: 27781559]
24. Xu L, Sheybani N, Ren S, Bowlin GL, Yeudall WA, Yang H. Semi-Interpenetrating Network (sIPN) Co-Electrospun Gelatin/Insulin Fiber Formulation for Transbuccal Insulin Delivery. Pharm Res. 2015; 32(1):275–85. [PubMed: 25030186]
25. Wu DW, Huang CC, Chang SW, Chen TH, Lee H. Bcl-2 stabilization by paxillin confers 5-fluorouracil resistance in colorectal cancer. Cell Death Differ. 2015; 22(5):779–89. [PubMed: 25323586]
26. Wang Y, Shi F, Xing GH, Xie P, Zhao N, Yin YF, Sun SY, He J, Xuan SY. Protein Regulator of Cytokinesis PRC1 Confers Chemoresistance and Predicts an Unfavorable Postoperative Survival of Hepatocellular Carcinoma Patients. J Cancer. 2017; 8(5):801–808. [PubMed: 28382142]
27. Workman P, Aboagye EO, Balkwill F, Balmain A, Bruder G, Chaplin DJ, Double JA, Everitt J, Farningham DA, Glennie MJ, Kelland LR, Robinson V, Stratford IJ, Tozer GM, Watson S, Wedge SR, Eccles SA. Guidelines for the welfare and use of animals in cancer research. Br J Cancer. 2010; 102(11):1555–77. [PubMed: 20502460]
28. Caruana I, Savoldo B, Hoyos V, Weber G, Liu H, Kim ES, Ittmann MM, Marchetti D, Dotti G. Heparanase promotes tumor infiltration and antitumor activity of CAR-redirected T lymphocytes. Nat Med. 2015; 21(5):524–9. [PubMed: 25849134]
29. Xu L, Yeudall WA, Yang H. Folic Acid-Decorated Polyamidoamine Dendrimer Exhibits High Tumor Uptake and Sustained Highly Localized Retention in Solid Tumors: Its Utility for Local siRNA Delivery. Acta biomaterialia. 2017
30. Zhang X, Bai Q, Kakiyama G, Xu L, Kim JK, Pandak WM Jr, Ren S. Cholesterol metabolite, 5-cholesten-3beta-25-diol-3-sulfate, promotes hepatic proliferation in mice. J Steroid Biochem Mol Biol. 2012; 132(3-5):262–70. [PubMed: 22732306]
31. Luong D, Kesharwani P, Deshmukh R, Mohd Amin MC, Gupta U, Greish K, Iyer AK. PEGylated PAMAM dendrimers: Enhancing efficacy and mitigating toxicity for effective anticancer drug and gene delivery. Acta Biomater. 2016; 43:14–29. [PubMed: 27422195]
32. Flanagan L, Meyer M, Fay J, Curry S, Bacon O, Duessmann H, John K, Boland KC, McNamara DA, Kay EW, Bantel H, Schulze-Bergkamen H, Prehn JH. Low levels of Caspase-3 predict favourable response to 5FU-based chemotherapy in advanced colorectal cancer: Caspase-3 inhibition as a therapeutic approach. Cell Death Dis. 2016; 7:e2087. [PubMed: 26844701]
33. Marin-Vicente C, Lyutvinskiy Y, Romans Fuertes P, Zubarev RA, Visa N. The effects of 5-fluorouracil on the proteome of colon cancer cells. J Proteome Res. 2013; 12(4):1969–79. [PubMed: 23477467]
34. Ooyama A, Oka T, Zhao HY, Yamamoto M, Akiyama S, Fukushima M. Anti-angiogenic effect of 5-Fluorouracil-based drugs against human colon cancer xenografts. Cancer Lett. 2008; 267(1):26–36. [PubMed: 18420342]
35. Norouzi M, Nazari B, Miller DW. Injectable hydrogel-based drug delivery systems for local cancer therapy. Drug Discov Today. 2016
36. Wang LL, Sloand JN, Gaffey AC, Venkataraman CM, Wang Z, Trubelja A, Hammer DA, Atluri P, Burdick JA. Injectable, Guest-Host Assembled Polyethylenimine Hydrogel for siRNA Delivery. Biomacromolecules. 2017; 18(1):77–86. [PubMed: 27997133]
37. Price R, Poursaid A, Cappello J, Ghandehari H. In vivo evaluation of matrix metalloproteinase responsive silk-elastinlike protein polymers for cancer gene therapy. J Control Release. 2015; 213:96–102. [PubMed: 26095079]
38. Li J, Gong C, Feng X, Zhou X, Xu X, Xie L, Wang R, Zhang D, Wang H, Deng P, Zhou M, Ji N, Zhou Y, Wang Y, Wang Z, Liao G, Geng N, Chu L, Qian Z, Wang Z, Chen Q. Biodegradable

thermosensitive hydrogel for SAHA and DDP delivery: therapeutic effects on oral squamous cell carcinoma xenografts. PLoS One. 2012; 7(4):e33860. [PubMed: 22529899]

39. Gustafson JA, Price RA, Greish K, Cappello J, Ghandehari H. Silk-elastin-like hydrogel improves the safety of adenovirus-mediated gene-directed enzyme-prodrug therapy. Mol Pharm. 2010; 7(4): 1050–6. [PubMed: 20586469]
40. Buczkowski A, Olesinski T, Zbicinska E, Urbaniak P, Palecz B. Spectroscopic and calorimetric studies of formation of the supramolecular complexes of PAMAM G5-NH(2) and G5-OH dendrimers with 5-fluorouracil in aqueous solution. International journal of pharmaceutics. 2015; 490(1-2):102–11. [PubMed: 25997661]
41. Buczkowski A, Waliszewski D, Urbaniak P, Palecz B. Study of the interactions of PAMAM G3-NH2 and G3-OH dendrimers with 5-fluorouracil in aqueous solutions. International journal of pharmaceutics. 2016; 505(1-2):1–13. [PubMed: 27039147]
42. Fourniols T, Randolph LD, Staub A, Vanvarenberg K, Leprince JG, Preat V, des Rieux A, Danhier F. Temozolomide-loaded photopolymerizable PEG-DMA-based hydrogel for the treatment of glioblastoma. J Control Release. 2015; 210:95–104. [PubMed: 25982679]
43. Obara K, Ishihara M, Ozeki Y, Ishizuka T, Hayashi T, Nakamura S, Saito Y, Yura H, Matsui T, Hattori H, Takase B, Ishihara M, Kikuchi M, Maehara T. Controlled release of paclitaxel from photocrosslinked chitosan hydrogels and its subsequent effect on subcutaneous tumor growth in mice. J Control Release. 2005; 110(1):79–89. [PubMed: 16289419]
44. Nickerson MT, Patel J, Heyd DV, Rousseau D, Paulson AT. Kinetic and mechanistic considerations in the gelation of genipin-crosslinked gelatin. Int J Biol Macromol. 2006; 39(4-5):298–302. [PubMed: 16797690]
45. Zhu W, Li Y, Liu L, Chen Y, Wang C, Xi F. Supramolecular hydrogels from cisplatin-loaded block copolymer nanoparticles and alpha-cyclodextrins with a stepwise delivery property. Biomacromolecules. 2010; 11(11):3086–92. [PubMed: 20958000]
46. Xu L, Zolotarskaya OY, Yeudall WA, Yang H. Click hybridization of immune cells and polyamidoamine dendrimers. Adv Healthc Mater. 2014; 3(9):1430–8. [PubMed: 24574321]
47. Baskin JM, Prescher JA, Laughlin ST, Agard NJ, Chang PV, Miller IA, Lo A, Codelli JA, Bertozzi CR. Copper-free click chemistry for dynamic in vivo imaging. Proc Natl Acad Sci U S A. 2007; 104(43):16793–7. [PubMed: 17942682]
48. Khaled SZ, Cevenini A, Yazdi IK, Parodi A, Evangelopoulos M, Corbo C, Scaria S, Hu Y, Haddix SG, Corradetti B, Salvatore F, Tasciotti E. One-pot synthesis of pH-responsive hybrid nanogel particles for the intracellular delivery of small interfering RNA. Biomaterials. 2016; 87:57–68. [PubMed: 26901429]
49. Lin Z, Gao W, Hu H, Ma K, He B, Dai W, Wang X, Wang J, Zhang X, Zhang Q. Novel thermo-sensitive hydrogel system with paclitaxel nanocrystals: High drug-loading, sustained drug release and extended local retention guaranteeing better efficacy and lower toxicity. J Control Release. 2014; 174:161–70. [PubMed: 24512789]
50. Wang W, Song H, Zhang J, Li P, Li C, Wang C, Kong D, Zhao Q. An injectable, thermosensitive and multicompartment hydrogel for simultaneous encapsulation and independent release of a drug cocktail as an effective combination therapy platform. J Control Release. 2015; 203:57–66. [PubMed: 25683618]
51. Huebsch N, Kearney CJ, Zhao X, Kim J, Cezar CA, Suo Z, Mooney DJ. Ultrasound-triggered disruption and self-healing of reversibly cross-linked hydrogels for drug delivery and enhanced chemotherapy. Proc Natl Acad Sci U S A. 2014; 111(27):9762–7. [PubMed: 24961369]
52. Mukerji R, Schaal J, Li X, Bhattacharyya J, Asai D, Zalutsky MR, Chilkoti A, Liu W. Spatiotemporally photoradiation-controlled intratumoral depot for combination of brachytherapy and photodynamic therapy for solid tumor. Biomaterials. 2016; 79:79–87. [PubMed: 26702586]

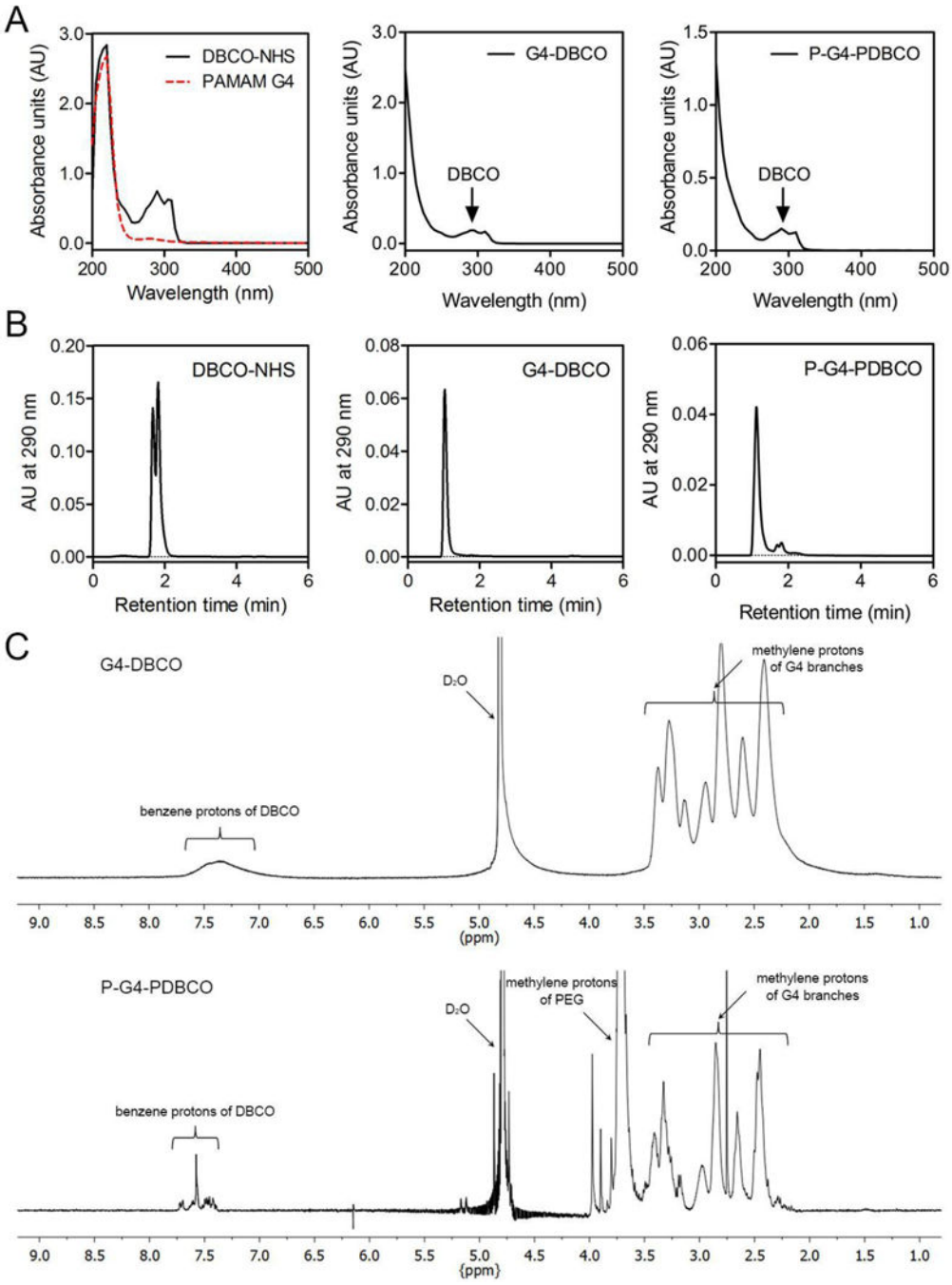

Figure 1.

Structure characterization of G4-DBCO and P-G4-PDBCO macromonomers. (A) The UV-Vis spectra of DBCO-NHS, PAMAM dendrimer G4, G4-DBCO and P-G4-PDBCO dendrimer conjugates. (B) HPLC chromatograms of DBCO-NHS, G4-DBCO, and P-G4-PDBCO. (C) ^{1}H NMR spectra of G4-DBCO and P-G4-PDBCO in D_2O.

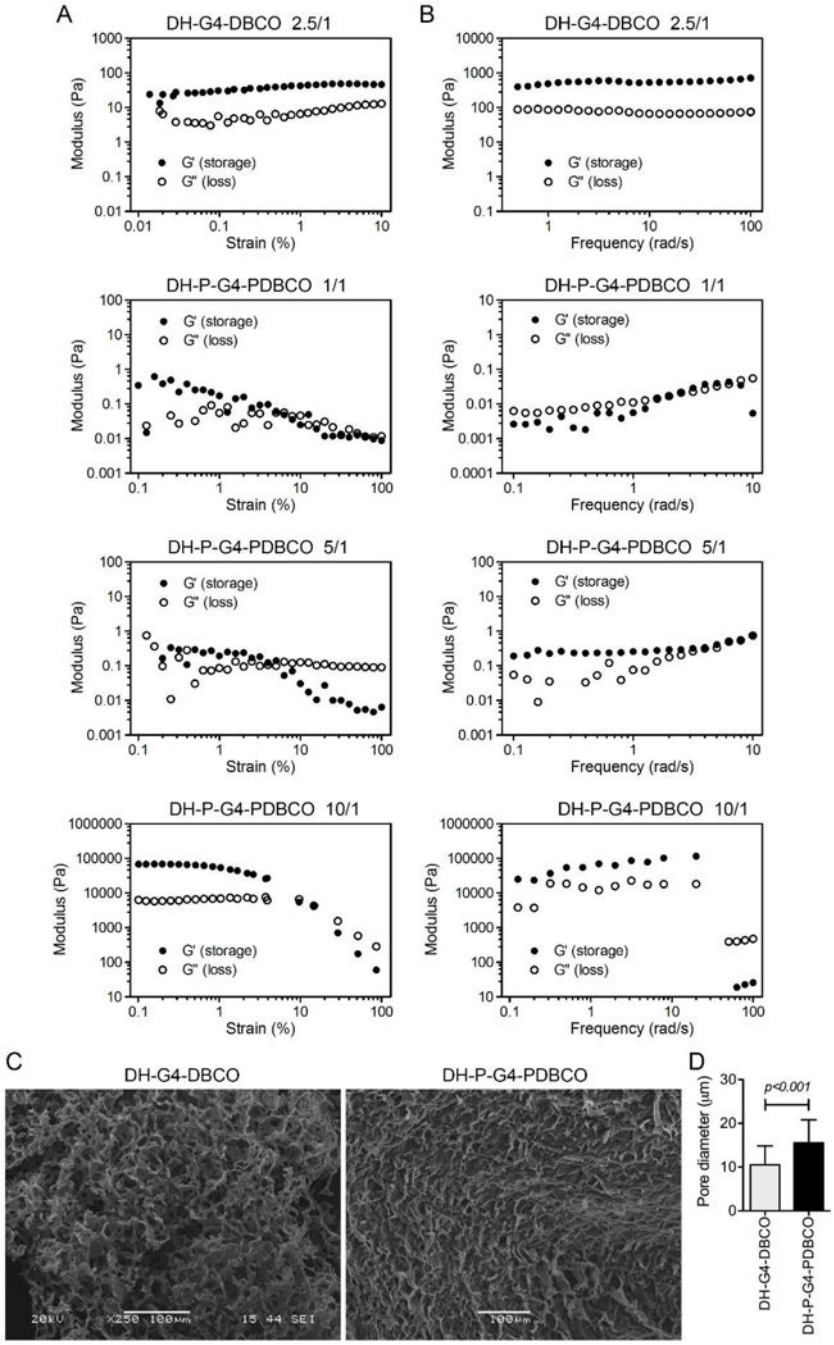

Figure 2.

Physical characterization of DH-G4-DBCO and DH-P-G4-PDBCO. Oscillatory amplitude sweep tests (A) and oscillatory frequency tests (B) of DHs as determined at weight ratio of PEG-BA/G4-DBCO=2.5/1 (DH-G4-DBCO) and PEG-BA/P-G4-PDBCO=1/1, 5/1 or 10/1 (DH-P-G4-PDBCO). (C) SEM images of DH-G4-DBCO and DH-P-G4-PDBCO with a microscopic network structure of the gel. (D) Apparent pore diameter of DH-G4-DBCO and DH-P-G4-PDBCO was quantified by Image J based on the SEM images.

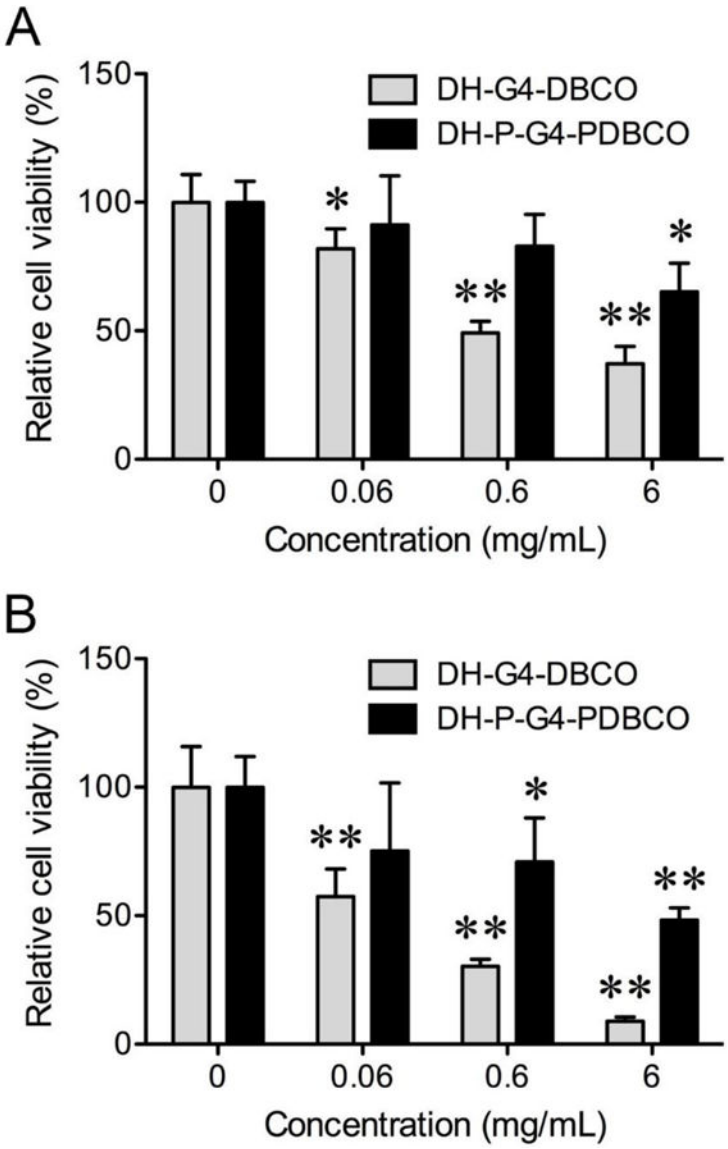

Figure 3.

Dose-dependent cytotoxicity of DH-G4-DBCO and DH-P-G4-PDBCO to HN12 cells (A) and NIH3T3 fibroblasts (B) as determined by WST-1 assay. The bars and error bars are means ± SD (n = 6). *$p < 0.05$ and **$p < 0.01$ versus no treatment (DH concentration at 0 mg/mL).

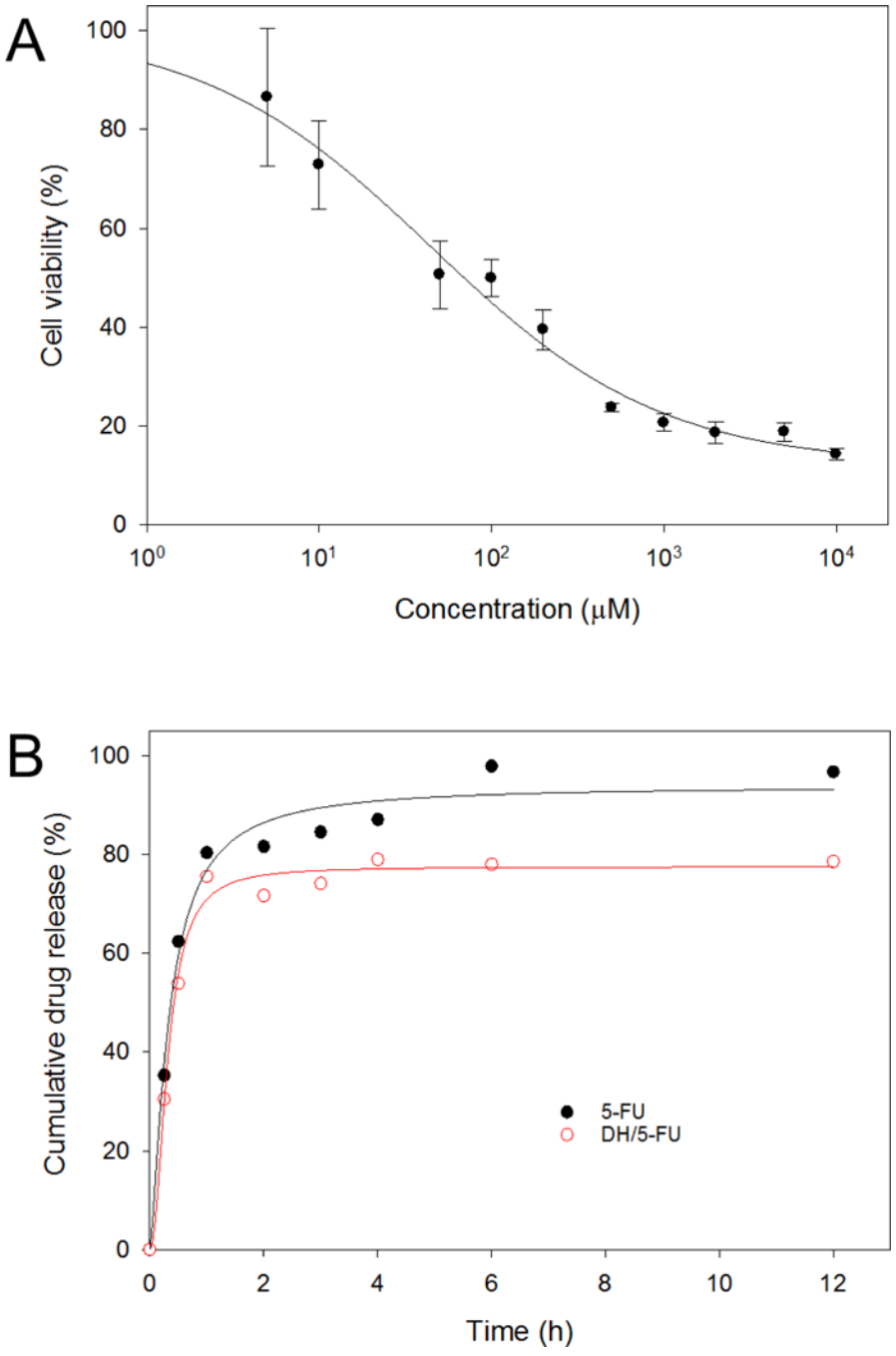

Figure 4.

In vitro activity and release kinetics of 5-FU. (A) Dose-dependent toxicity of 5-FU to HN12 cells. (B) Extended release of 5-FU from DH-P-G4-PDBCO (DH).

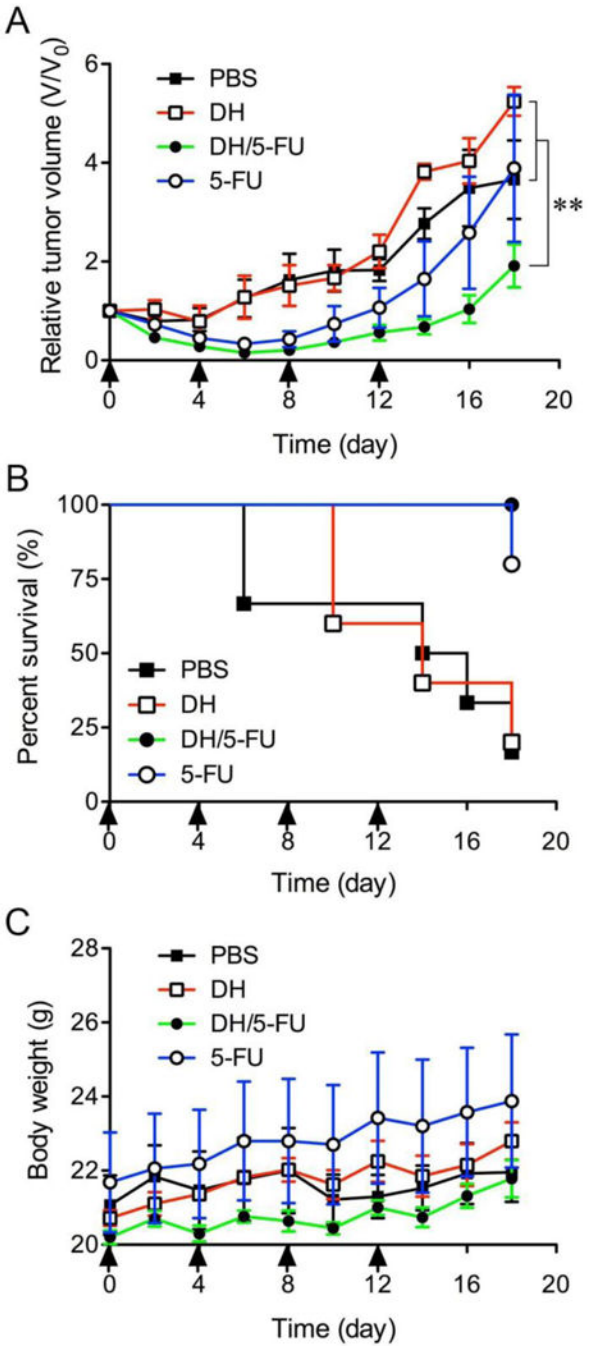

Figure 5.

In vivo assessment of antitumor effects of DH/5-FU. (A) Change of relative tumor volume [ratio of mouse tumor volume (V) to initial tumor (V_0)] was monitored over the course of treatment. (B) The survival was estimated by using Kaplan–Meier analysis. (C) Body weights of mice in all groups were recorded. Arrow bars indicate the days when the mice were given injection. ** $p < 0.01$ vs. the PBS and DH groups.

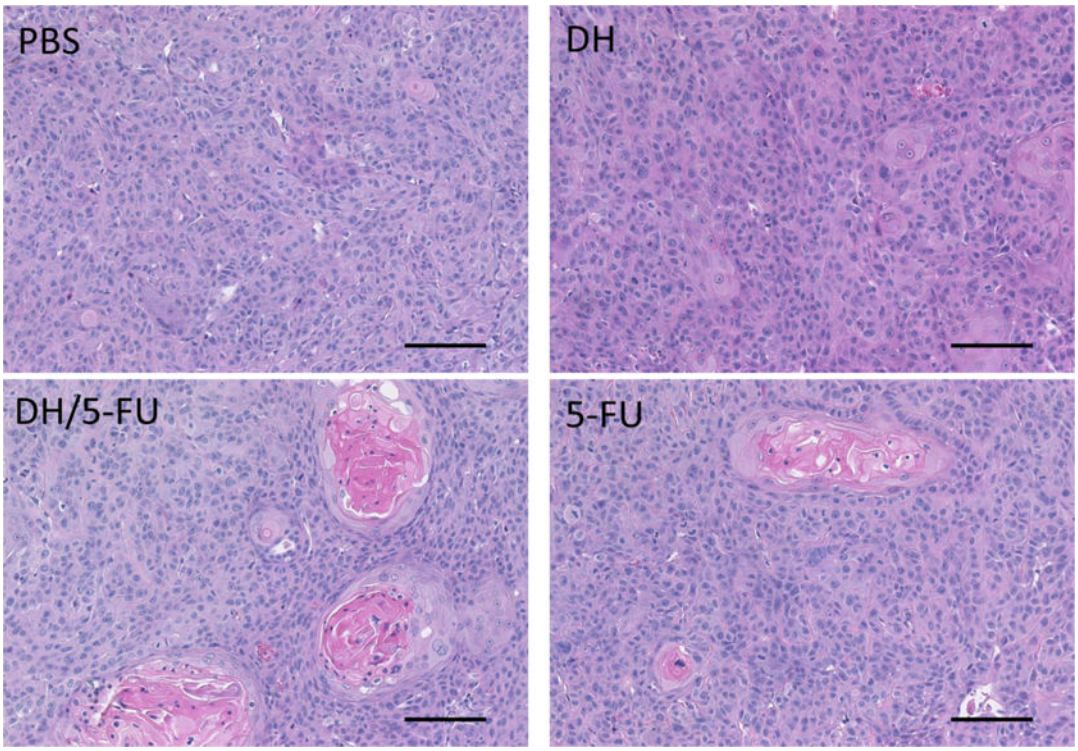

Figure 6.
Representative images of H&E staining of the tumor sections. Scale bar: 100 μm.

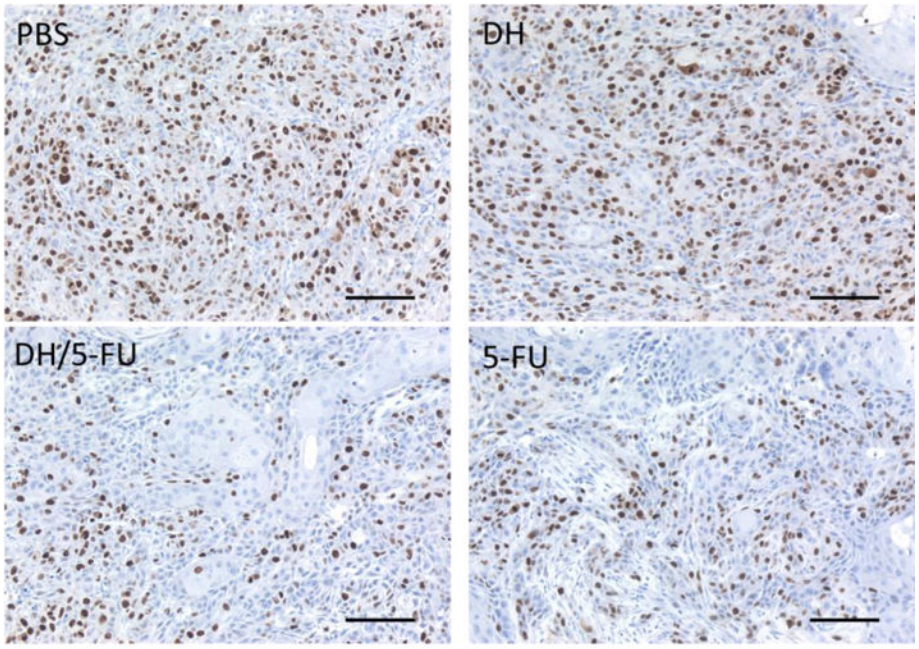

A

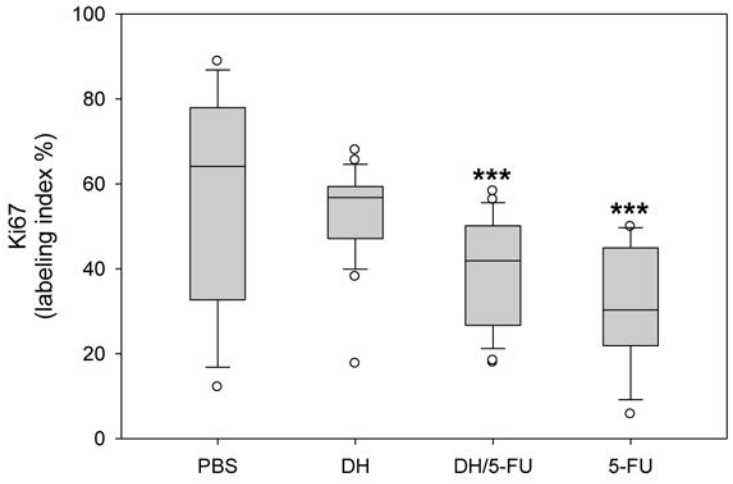

B

Figure 7.

IHC staining of Ki67, a marker of proliferating cells in the tumor sections. (A) Representative images. Scale bar: 100 μm. (B) Fractions of Ki67-positive cells. *** p<0.001 vs. the PBS group.

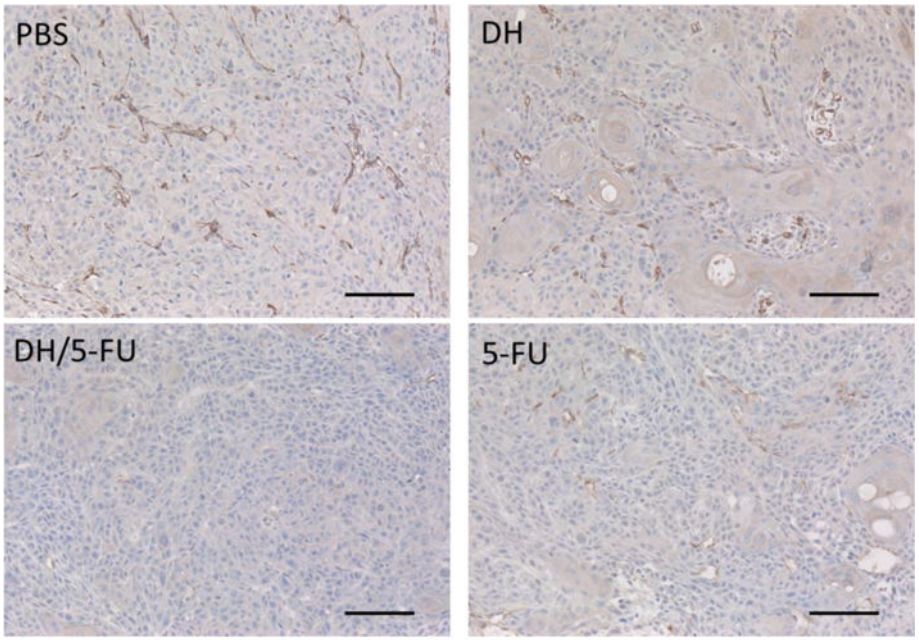

A

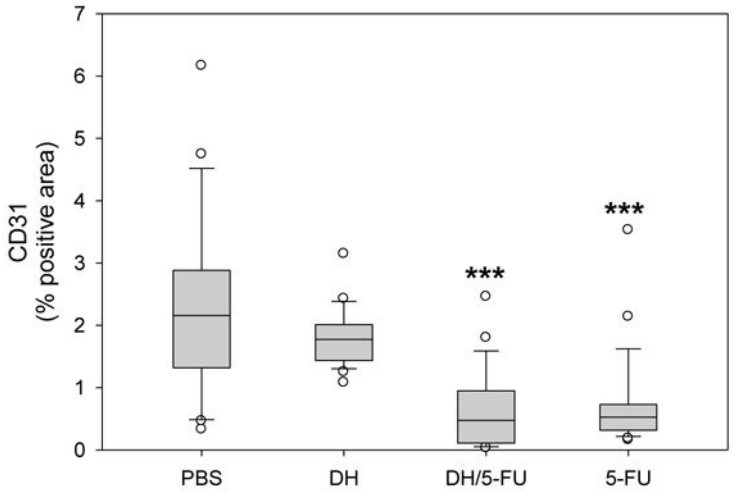

B

Figure 8.

IHC staining of CD31, a marker of angiogenesis in the tumor sections. (A) Representative images. Scale bar: 100 μm. (B) Fractions of CD31-positive areas in the tumor sections. *** p<0.001 vs. the PBS group.

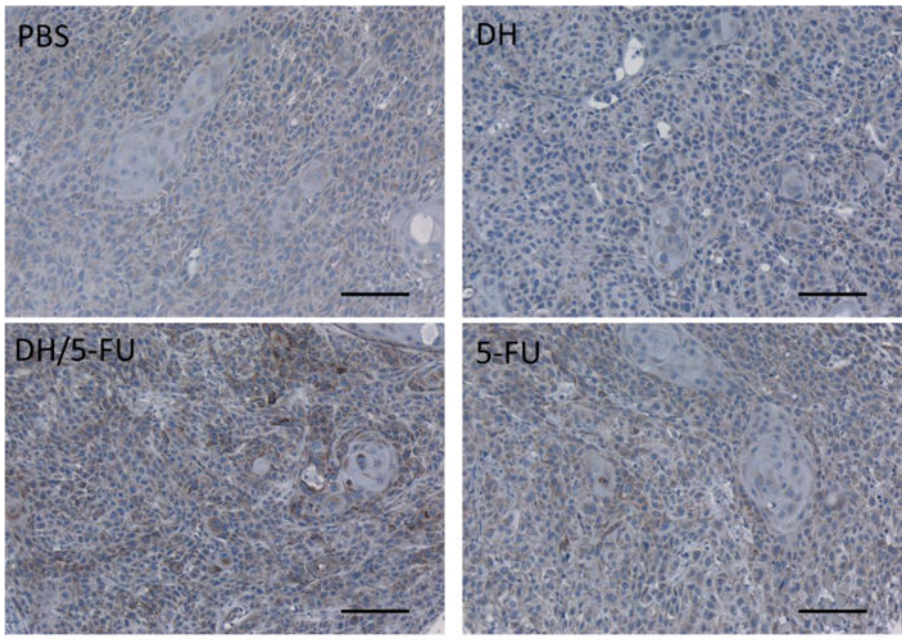

A

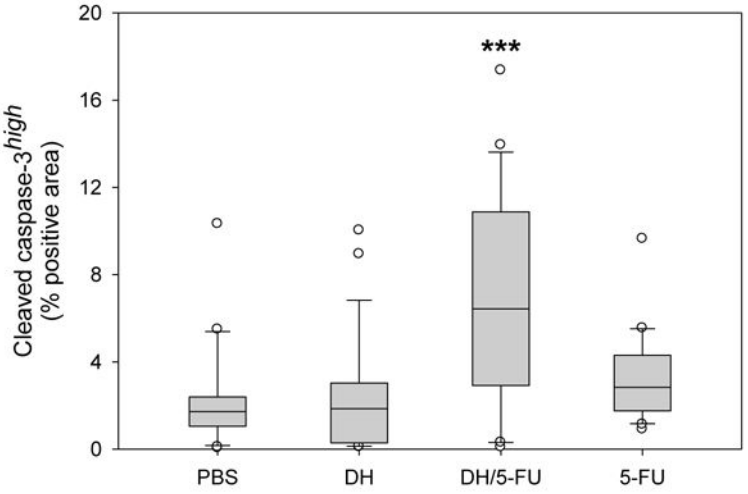

B

Figure 9.

IHC staining of cleaved caspase-3, a marker of apoptosis in the tumor sections. (A) Representative images. Scale bar: 100 μm. (B) Fractions of cleaved caspase-3^{high} cells in the tumor sections. *** $p<0.001$ vs. the PBS group.

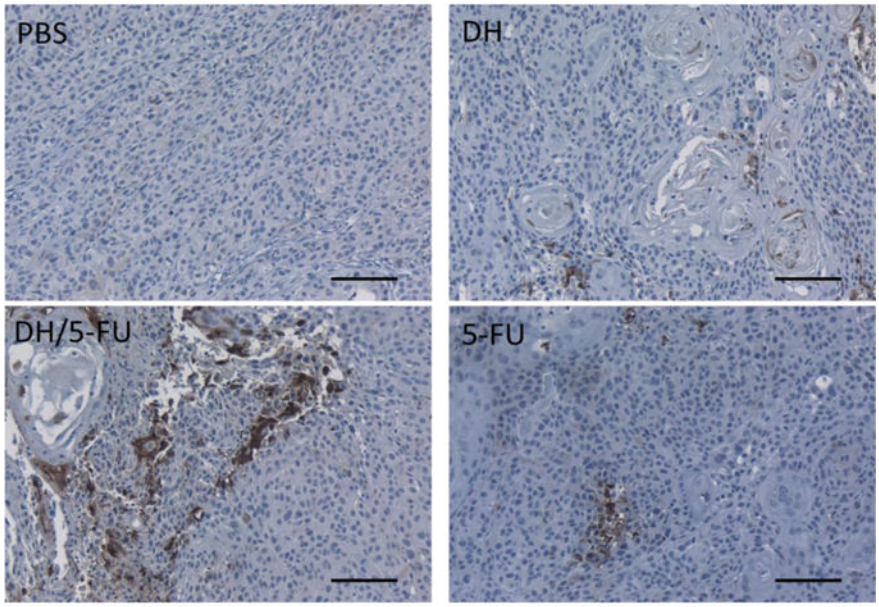

A

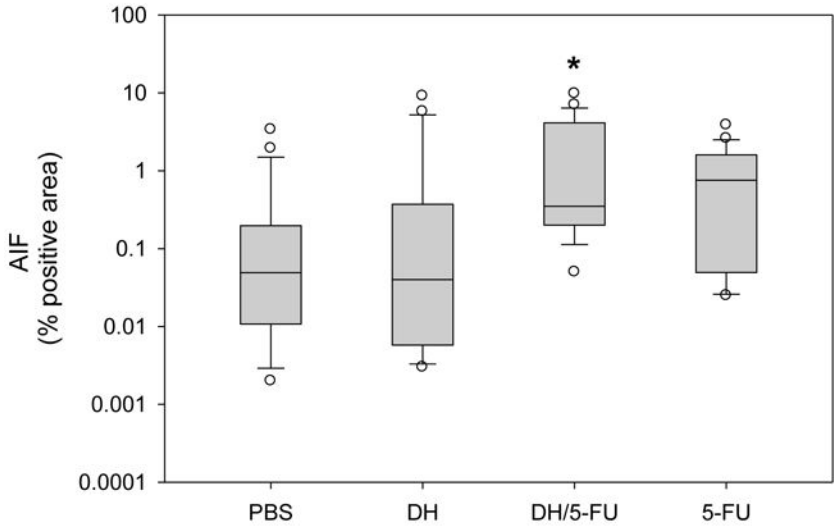

B

Figure 10.

IHC staining of apoptosis-inducing factor (AIF), a marker of apoptosis in the tumor sections. (A) Representative images. Scale bar: 100 μm. (B) Fractions of AIF-positive cells in the tumor sections. * $p < 0.05$ vs. the PBS group.

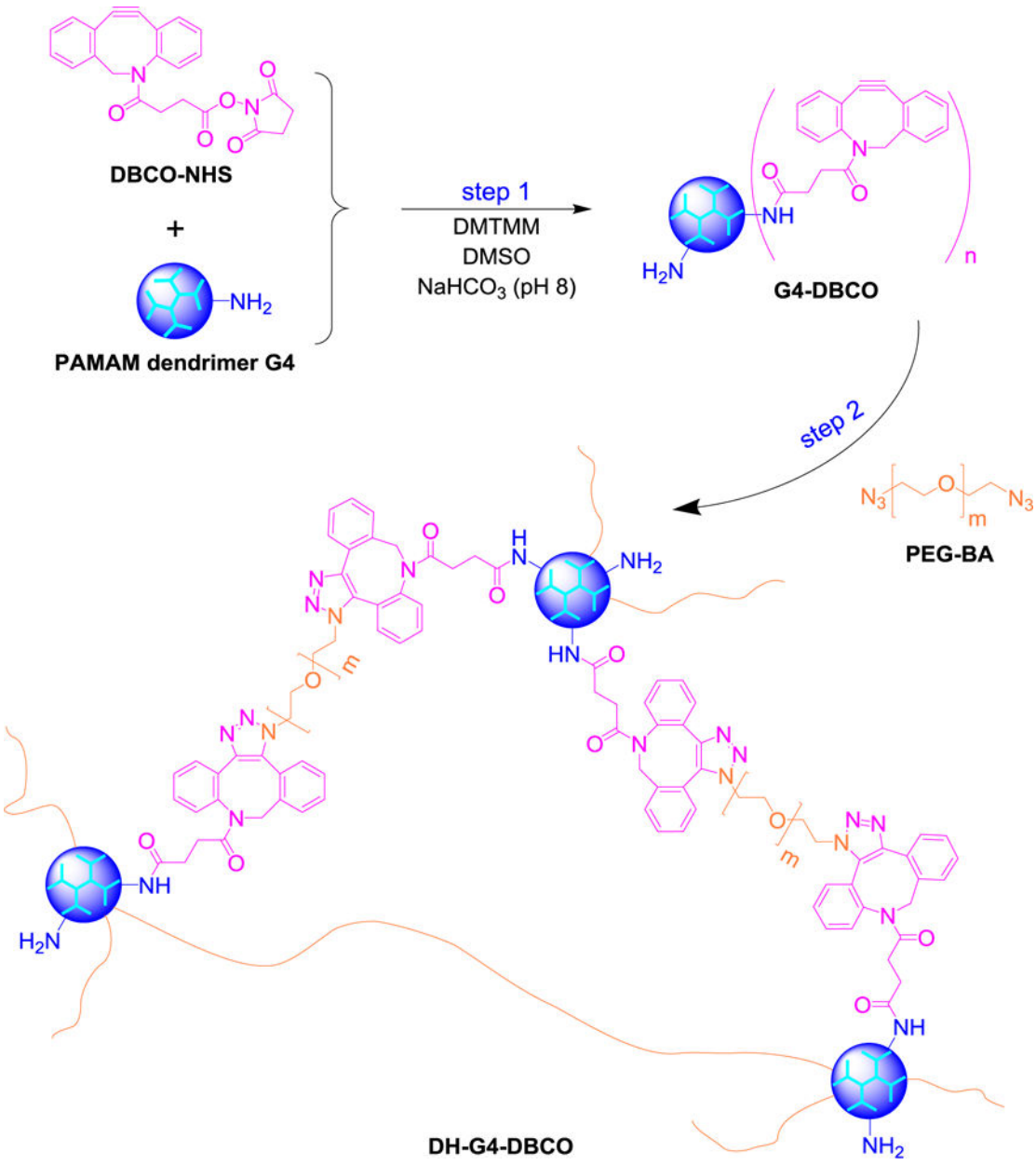

Scheme 1.
Synthesis of bioorthogonal dendrimer hydrogel DH-G4-DBCO.

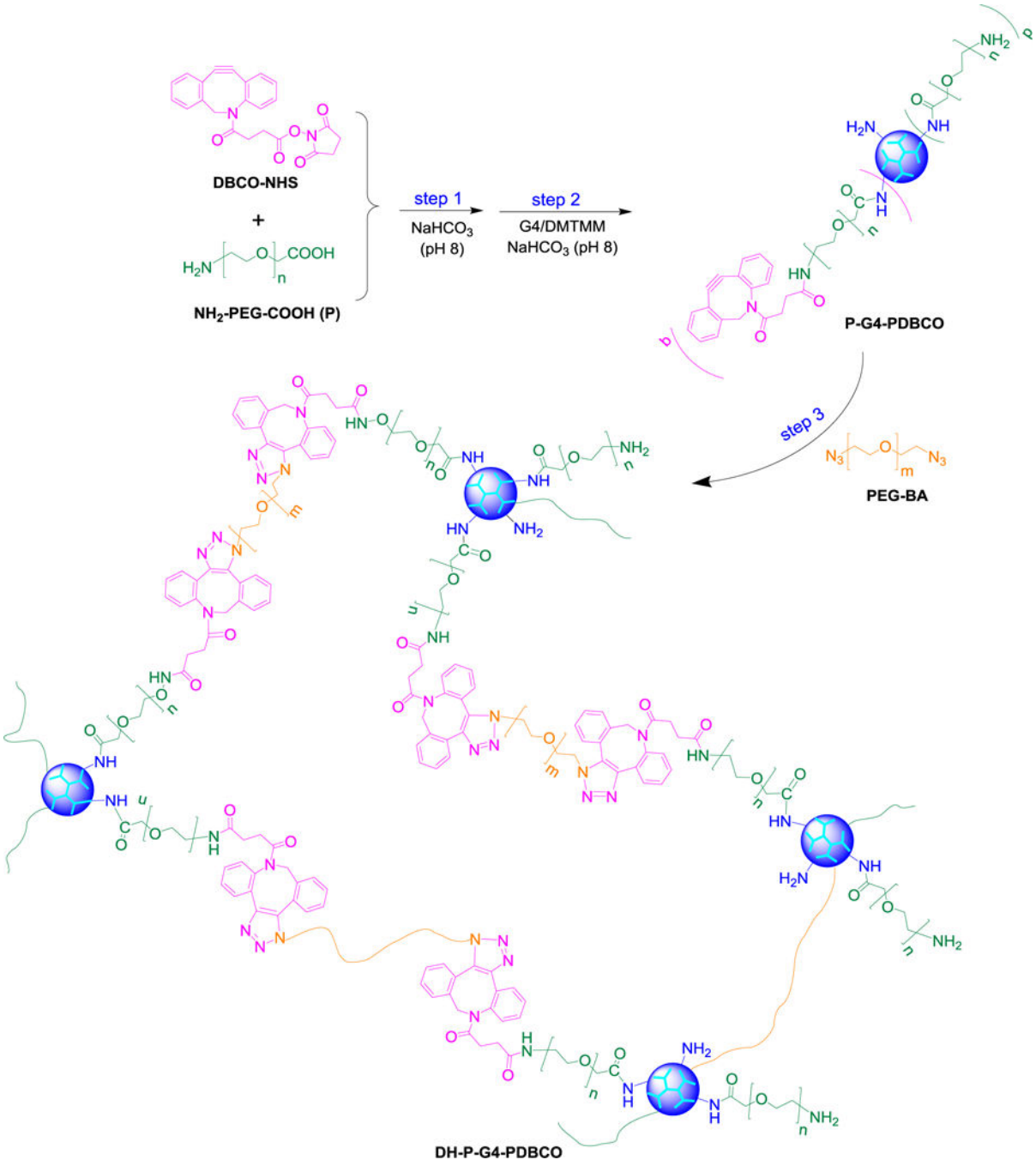

Scheme 2.
Synthesis of bioorthogonal dendrimer hydrogel DH-P-G4-PDBCO.